How to cite: *Angew. Chem. Int. Ed.* **2023**, *62*, e202313540
doi.org/10.1002/anie.202313540

Carbon Nitride

Singlet-Triplet Energy Inversion in Carbon Nitride Photocatalysts

*Arianna Actis, Michele Melchionna, Giacomo Filippini, Paolo Fornasiero, Maurizio Prato, Mario Chiesa, and Enrico Salvadori**

Abstract: Time-resolved EPR (TR-EPR) demonstrates the formation of well-defined spin triplet excitons in carbon nitride. This permits to experimentally probe the extent of the triplet wavefunction which delocalizes over several tri-*s*-triazine units. Analysis of the temperature dependence of the TR-EPR signal reveals the mobility of the triplet excitons. By employing monochromatic light excitation in the range 430–600 nm, the energy of the spin triplet is estimated to be ≈0.2 eV above the conduction band edge, proving that the triplet exciton lies above the corresponding singlet. Comparison between amorphous and graphitic forms establishes the singlet-triplet inversion as a general feature of carbon nitride materials.

In this communication, the properties of spin triplet excitons in carbon nitride are directly probed by means of time-resolved electron paramagnetic resonance (TR-EPR) spectroscopy. These properties include extent of wavefunction delocalization, energy and mobility. We focus on the catalytically relevant amorphous form and compare to the conventionally prepared graphitic one to demonstrate that the energy of the photoexcited singlet exciton lies below that of the corresponding triplet.

Carbon nitride (CN) is a polymeric semiconductor with graphite-like structure, in which the alternating sp^2 carbon and nitrogen atoms of tri-*s*-triazine ($C_6N_7H_3$) form a highly π-conjugated electronic system. Adjacent tri-*s*-triazine units are connected at their corners by nitrogen atoms to yield the extended bi-dimensional structure. CN is sought after for its ability to catalyze a wide scope of chemical reactions by harnessing visible light.[1,2,3,4] Because of its cost-effective preparation and flexibility to be structurally tuned towards a range of photocatalytic reactions, CN has attracted widespread attention in recent years, becoming undoubtedly one of the most rapidly emerging new semiconductors in photocatalysis.

CN is characterized by a narrow band gap of 2.5–2.7 eV depending on the preparation and post-synthetic treatments, therefore electron-hole pairs can be easily formed by light with wavelength <460 nm. In most semiconductors these photogenerated charge carriers can be considered as independent, however, the low dielectric constant of CN makes the Coulombic interaction between charges strong enough to lead to the formation of bound electron-hole pairs, also known as excitons.[5] Because they are strongly correlated, such excitons may exist either in a singlet or a triplet state configuration. Spin triplet states are central in defining the photochemistry of a material as they usually possess a relatively long lifetime (due to spin-forbidden recombination) that supports reactivity on the timescale of diffusion. Species whose lifetime spans the ns-ms timescale are highly relevant, in particular for photocatalysis, as they: (*i*) are compatible with chemical reactions occurring at the surface (Figure 1a), (*ii*) are more likely to evolve to free charge carriers, able to prompt redox reactions[6,7,8] or (*iii*) to localize at defect sites to form other reactive species.[9,10] All these properties justify the intense interest for maximising triplet harvesting, for instance by singlet fission in organic photovoltaics solar cells[11] or singlet-triplet and triplet-triplet annihilation in OLEDs.[12] A desirable feature on the way to increase the yield of triplet formation is a small singlet-triplet exchange energy, which promotes efficient conversion between singlet and triplet excitons. Such a small exchange energy is readily achievable when the highest occupied (HOMO) and lowest unoccupied molecular orbitals (LUMO) are spatially nonoverlapping, yielding a charge-transfer excited state.[13,14] This results in a peculiar energy arrangement of the excited singlet and triplet states, with the former being at lower energy, an exception to Hund's rule. This singlet-triplet energy inversion was recently

[*] A. Actis, Prof. Dr. M. Chiesa, Prof. Dr. E. Salvadori
Department of Chemistry and NIS Centre,
University of Torino
Via Pietro Giuria 7, 10125 Torino (Italy)
E-mail: enrico.salvadori@unito.it
Prof. Dr. M. Melchionna, Dr. G. Filippini, Prof. Dr. P. Fornasiero, Prof. Dr. M. Prato
Department of Chemical and Pharmaceutical, INSTM UdR,
University of Trieste
Via Licio Giorgieri 1, 34127 Trieste (Italy)
Prof. Dr. P. Fornasiero
ICCOM-CNR URT, Via Licio Giorgieri 1, 34127 Trieste (Italy)
Prof. Dr. M. Prato
Center for Cooperative Research in Biomaterials (CIC biomaGUNE),
Basque Research and Technology Alliance (BRTA)
Paseo Miramon 194, 20014 Donostia San Sebastián (Spain)
Prof. Dr. M. Prato
Basque Fdn Sci
Ikerbasque, 48013 Bilbao (Spain)

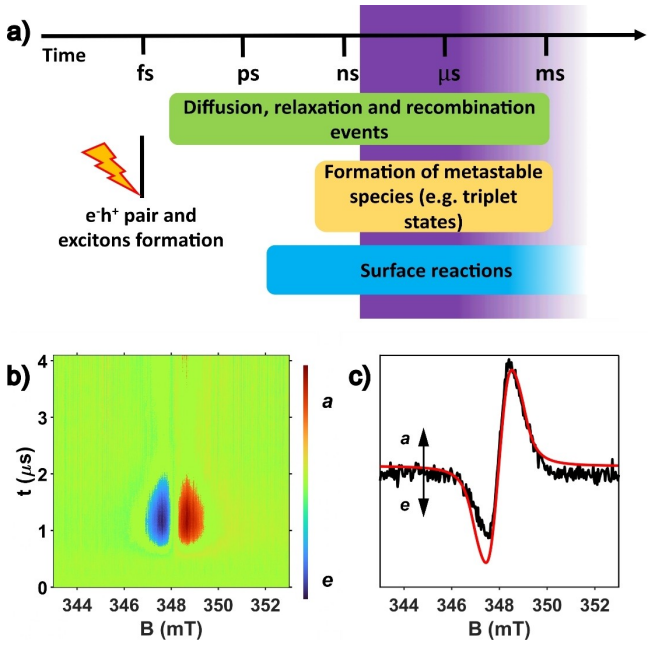

Figure 1. a) Timescales of physical and chemical processes characteristic of semiconducting photocatalysts. The region shaded in purple represent the timescale accessible through TR-EPR. b) TR-EPR surface recorded on am-CN under 355 nm laser irradiation at 50 K, c) triplet state EPR spectrum extracted from *b* by integrating from 1.0 to 1.3 µs. *a* = enhanced absorption, *e* = emission.

demonstrated for substituted tri-*s*-triazine,[15] the basic unit of carbon nitride.

To understand whether singlet-triplet inversion occurs also in polymerized bulk CN, we employed EPR spectroscopy in its time-resolved form. TR-EPR is a highly sensitive spectroscopic technique that provides clear-cut evidence for the presence of metastable and polarized high-spin states.[16,17] The characteristic signal shows components in enhanced absorption (*a*) and/or emission (*e*). In defining the photophysics of complex inorganic semiconductors, the key advantage of TR-EPR is its selectivity for paramagnetic states and the ability to unambiguously assign the spin multiplicity of transient species, thus outperforming optical spectroscopy in this task.[17] Moreover, since TR-EPR detects the formation of transient species through their magnetic and not optical properties, this technique is not affected by the limitation of optical spectroscopy (e.g., light scattering) and can be performed on bulk samples, avoiding the need of bespoke CN samples that differ from those used in catalysis.[4]

It must be pointed out that the generic name of carbon nitride includes a rather broad family of materials, varying in terms of structure and composition. Such variations may heavily impact the photophysics of the material and, ultimately, its photochemistry.[4,18] Recent findings revealed that a less crystalline CN derivative (amorphous CN, am-CN) exhibits a superior photocatalytic activity in a class of organic reactions based on C–C couplings with perfluoroalkyl derivatives (Figure S1).[19,20] Herein, we therefore focus on the singlet-triplet inversion in am-CN in order to understand how this can potentially impact other classes of reactions featuring similar mechanistic steps.

Figure 1b reports the 2D experimental TR-EPR contour plot for am-CN acquired after a 355 nm laser pulse (7 ns, 2 mJ) at $T = 50$ K. From this surface the characteristic spin-polarized triplet spectrum can be extracted (Figure 1c), demonstrating the formation of a well-defined triplet exciton. The spectrum is relatively narrow with a field span of ≈5 mT (from 345 to 350 mT) and can be satisfactorily simulated as a single spin triplet ($S = 1$) with characteristic zero-field splitting parameters $D = 30$ MHz and $E = 3$ MHz, and zero-field populations $P_X : P_Y : P_Z = 1 : 0.6 : 0$ (Figure S2).

In the framework of the point-dipole approximation, the value of D is proportional to (r^{-3}), where r is the average distance between the two unpaired electrons, and then can be exploited to estimate the extent of the spin delocalization,[17] see Supporting Information Section S1. The measured D value of 30 MHz would correspond to an average distance of ≈1.2 nm which, albeit a rough estimate and a lower-bound limit due to the extensive delocalization,[17,21,22] is consistent with the size of three tri-*s*-triazine units, Figure 2a.[23] This is at variance with the singlet exciton which appears to be localized over a single tri-*s*-triazine unit.[24,25] It is to note that localization of the triplet exciton on a single tri-*s*-triazine unit (0.68 nm) would lead to a D of 165 MHz (Supporting Information Section S1), that is more than five times larger than the experimental value.

Comparing the TR-EPR spectra recorded in the interval between 20 K and room temperature allows the estimation of the temperature dependence, due either to dynamic[17] or delocalization effects,[26] of the triplet wavefunction (Figure 2b). The width of the spectrum is constant in the range 20–50 K, while it decreases at room temperature by a factor of two ($D = 13$ MHz, $E = 3$ MHz, Table 1 and Table S1), providing a robust and specific indication that triplet excitons are essential features of the photophysics of CN and are substantially delocalized at room temperature (Figure S3).

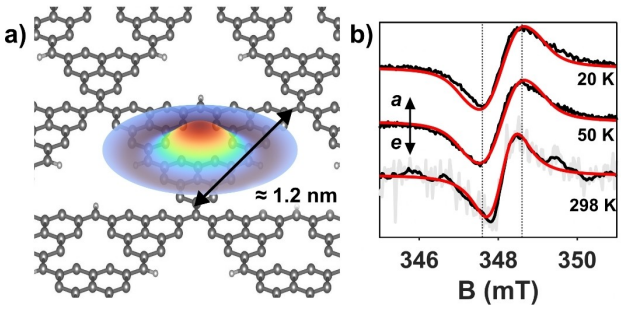

Figure 2. a) Pictorial representation of the spin triplet exciton delocalization over a single sheet of CN. b) TR-EPR spectra recorded on am-CN at 20 K, 50 K and 298 K and 460 nm irradiation, obtained by integration from 1.0 to 1.3 µs. The vertical lines are a guide to the eye to showcase the reduction of the spectral width. *a* = enhanced absorption, *e* = emission. The simulation parameters are reported in Table 1 and Table S1.

Table 1: Simulation parameters for the TR-EPR spectra reported in Figure 2b.[a]

Temperature	*D*	*E*	$P_x : P_y : P_z$
20	30	3	1 : 0.6 : 0
50	30	3	1 : 0.6 : 0
298	13	3	1 : 0.6 : 0

[a] Temperature is reported in Kelvin (K) and the zero-field splitting parameters (*D*, *E*) in MHz. g was assumed isotropic and equal to g_e (2.0032). The full set of parameters and relative errors is reported in Table S1.

To gain insights into the processes leading to the formation of the triplet exciton, we combined steady-state optical spectroscopy with photoluminescence spectroscopy and wavelength-dependent TR-EPR.

Figure 3 reports the diffuse reflectance UV/Vis (DR-UV/Vis) spectrum for am-CN, which displays the usual strong absorption below 450 nm and a composite tail between 450 and 600 nm (Figure S4). From the Tauc plot analysis (Figure S5) a band gap of 2.5 eV (=495 nm) can be estimated. To ascertain the origin of the metastable triplet exciton and whether it involves the band edges or intragap states we explored monochromatic wavelength excitations in the region spanning 430 to 600 nm around the band gap. All TR-EPR spectra, although varying in intensity, display a virtually identical shape regardless of the wavelength employed (Figure S6) and can be satisfactorily simulated with the same set of parameters used for the excitation at 355 nm, suggesting that only one main triplet exciton is formed. However, given the structural complexity of am-CN, it cannot be ruled out that minor differences that do not exceed the signal-to-noise may be present or that the observed triplet is the lowest in energy within the triplet manifold.[27] Magnetic interaction between two or more spin triplet cannot be excluded, however we do not have any evidence for the formation of higher spin states ($S>1$) under the experimental conditions adopted.

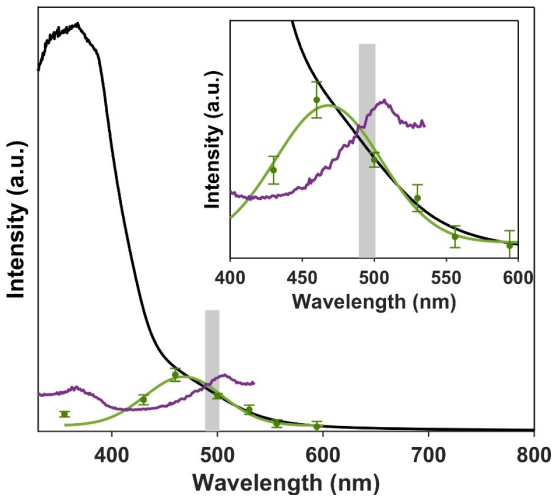

Figure 3. DR-UV/Vis spectrum of am-CN (black), photoluminescence excitation profile (purple), wavelength-dependent triplet exciton intensity (symbols) and the corresponding Gaussian fitting (green). The grey bar represents the band gap of am-CN (2.5 eV).

Fitting the TR-EPR intensity as a function of the excitation wavelength with a Gaussian yields a profile with maximum intensity at 460 nm (see Supporting Information), that encompasses the absorption shoulders visible in the DR-UV/Vis spectrum (Figure S4). Experimentally the intensity of a metastable triplet spectrum mainly depends on the triplet quantum yield (which can be taken to be constant) and the molar extinction coefficient at the excitation wavelength.[17] Therefore, the profile of the TR-EPR triplet signal intensity as a function of excitation wavelength should follow that of the DR-UV/Vis spectrum. In this instance, the TR-EPR spectrum collected at 430 nm has lower intensity than the corresponding spectrum collected at 460 nm, although the absorbance is significantly different (Figure 3). To understand this behavior, we have taken a complementary approach and considered the photoluminescence excitation spectrum of am-CN. This provides information on the singlet energy transfer pathways within the material, as this measurement reports on the conversion efficiency of the excitation energy into emission energy. Figure 3 (purple line) shows the excitation spectrum collected at the maximum of the photoluminescence emission (550 nm, Figure S7) while scanning the range 240 to 535 nm. The excitation spectrum does not closely follow the profile of the DR-UV/Vis but rather shows distinctive features: i) the region below 380 nm is not the most intense; and ii) the region between 380 and 480 nm presents a minimum in photoluminescence yield which corresponds (anti-correlate) to the maximum of the TR-EPR triplet intensity profile. Taken together these observations suggest that after excitation above the band gap, several deactivation pathways are available (photoluminescence, singlet-triplet conversion, non-radiative recombination, etc.) and that radiative recombination is not the preferred outcome, whereas excitation close to and below the band gap allows to directly access the metastable spin triplet.

Computational studies and optical spectroscopy data have suggested that tri-*s*-triazines present a peculiar singlet-triplet inversion ($E_{Triplet} > E_{Singlet}$) which dominates its photophysical response.[15,28,29,30] Further computations indicate that this energy inversion may also occur for CN, i.e. polymerized tri-*s*-triazine.[15] The TR-EPR data presented here support this prediction and place the triplet excitation energy at ≈2.7 eV above the valence band,[31] which is larger than the 2.5 eV estimated for the optical band gap (Figure 4). Moreover, the triplet absorption band, as reconstructed from TR-EPR measurements, suggests an energy spread for the triplet exciton of ≈0.6 eV (full width half maximum), whereas, as previously described,[32] photoluminescence measurements permit to estimate the spread of the emissive singlet states which extend from the conduction band to 0.3 eV beneath, Figure S8. This is schematically shown in Figure 4 which reports the analogue of a Jablonski diagram for this solid-state semiconductor (Figure 4a) and the experimental data employed to construct it (Figure 4b).

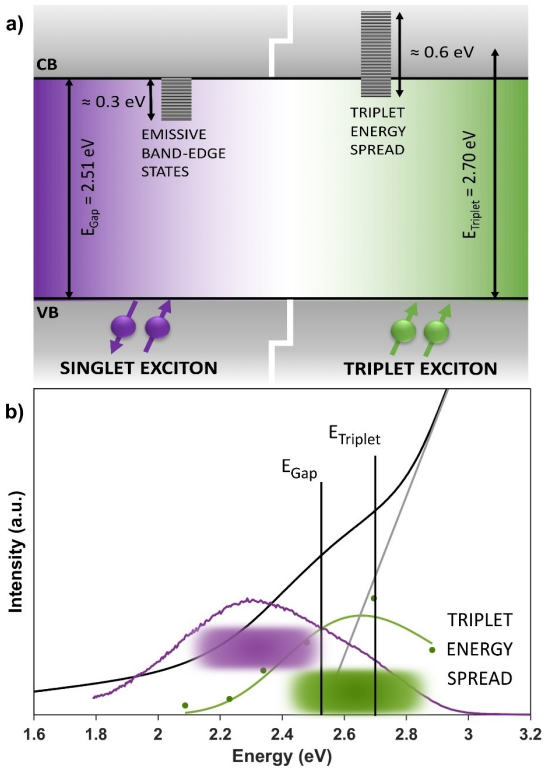

Figure 4. a) Schematic representation of the states determining the photophysics of CN and their energies gaps for the singlet and triplet manifolds. b) Absorption (black) and photoluminescence (purple) spectra of am-CN and triplet absorption band displayed on the energy scale. The position of the band gap (Tauc fitting in grey) and the triplet maximum are indicated as well as the energy spread for the triplet exciton (green shaded area) and of the emissive band edge states (purple shaded area).

These findings make singlet and triple excitons almost isoenergetic, which likely favours the singlet-triplet conversion in this semiconductor.

Finally, it is worth noting that the formation of photo-excited triplet excitons in CN is not related to the specific morphology of the material, as a similar TR-EPR spectrum, is observed also for the graphitic material (g-CN, Figure S9). Moreover, analysis of the triplet excitons in g-CN suggests that singlet and triplet excitons are inverted regardless of the morphology (Supporting Information Figures S10 and S11). It appears therefore than the formation of photo-excited triplet excitons is an intrinsic feature of CN, whereas the photocatalytic activity depends on the energy landscape related to the specific morphological and defective structure of the material.[10,19]

In conclusion, we have demonstrated the capability of TR-EPR in elucidating central details in the photochemistry of polycrystalline inorganic solids. Specifically, photoexcitation of am-CN in the range 355–600 nm results in the formation of a well-defined but delocalised spin triplet exciton whose energy lies above the band gap. Together with steady state optical spectroscopy, these observations demonstrate that singlet and triplet excitons are inverted by ≈0.2 eV. Since the triplet exciton is higher in energy than the singlet it cannot constitute an energy loss mechanism and all the absorbed photon energy is preserved and can efficiently drive photo-reactivity. Moreover, the easy inter-conversion between triplet-singlet spin configurations may explain the long photoluminescence lifetimes observed for CN materials.

Supporting Information

The authors have cited additional references within the Supporting Information.[33,45]

Acknowledgements

M. C. and E. S. acknowledge support through the Project CH4.0 under the MUR program "Dipartimenti di Eccellenza 2023–2027" (CUP: D13C22003520001). M. C. and P. F. acknowledge funding from MUR through the project SySSy-Cat (PRIN 2022, 20224P9ABM; CUP: J53D23008460006), while M. P. Acknowledges funding from MUR through the project (PRIN2022, 20228YFRNL). M. M. and G. F. kindly acknowledge FRA 2022 funded by the University of Trieste and Microgrants 2021 funded by Region FVG (LR 2/2011, ART. 4).

Conflict of Interest

The authors declare no conflict of interest.

Data Availability Statement

The data that support the findings of this study are available from the corresponding author upon reasonable request.

Keywords: Carbon Nitride · EPR Spectroscopy · Photochemistry · Time-Resolved EPR · Triplet State

[1] Q. Cao, B. Kumur, M. Antonietti, B. V. K. J. Schmidt, *Mater. Horiz.* **2020**, *7*, 762–786.
[2] A. Savateev, I. Ghosh, B. König, M. Antonietti, *Angew. Chem. Int. Ed.* **2018**, *57*, 15936–15947.
[3] J. Liu, W. Hongqjang, M. Antonietti, *Chem. Soc. Rev.* **2016**, *45*, 2308–232.
[4] V. W. Lau, B. V. Lotsch, *Adv. Energy Mater.* **2022**, *12*, 2101078.
[5] Y. Li, S. Jin, X. Xu, H. Wang, X. Zhang, *J. Appl. Phys.* **2020**, *127*, 170903.
[6] A. Savateev, N. V. Tarakina, V. Strauss, T. Hussain, K. ten Brummelhuis, J. M. Sánchez Vadillo, Y. Markushyna, S. Mazzanti, A. P. Tyutyunnik, R. Walczak, M. Oschatz, D. M. Guldi, A. Karton, M. Antonietti, *Angew. Chem. Int. Ed.* **2020**, *59*, 15061.
[7] A. J. Rieth, Y. Qin, B. C. M. Martindale, D. G. Nocera, *J. Am. Chem. Soc.* **2021**, *143*, 4646–4652.
[8] F. Strieth-Kalthoff, F. Glorius, *Chem* **2020**, *6*, 1888–1903.

[9] E. Raciti, S. M. Gali, M. Melchionna, G. Filippini, A. Actis, M. Chiesa, M. Bevilacqua, P. Fornasiero, M. Prato, D. Beljonne, R. Lazzaroni, *Chem. Sci.* **2022**, *13*, 9927–9939.
[10] A. Actis, M. Melchionna, G. Filippini, P. Fornasiero, M. Prato, E. Salvadori, M. Chiesa, *Angew. Chem. Int. Ed.* **2022**, *61*, e202210640.
[11] K. Miyata, F. S. Conrad-Burton, F. L. Geyer, X.-Y. Zhu, *Chem. Rev.* **2019**, *119*, 4261–4292.
[12] B. H. Drummond, N. Aizawa, Y. Zhang, W. K. Myers, Y. Xiong, M. W. Cooper, S. Barlow, Q. Gu, L. R. Weiss, A. J. Gillett, D. Credgington, Y.-J. Pu, S. R. Marder, E. W. Evans, *Nat. Commun.* **2021**, *12*, 4532.
[13] E. R. Bittner, V. Lankevich, S. Gelinas, A. Rao, D. A. Ginger, R. H. Friend, *Phys. Chem. Chem. Phys.* **2014**, *16*, 20321–20328.
[14] S. Difley, D. Beljonne, T. Van Voorhis, *J. Am. Chem. Soc.* **2008**, *130*, 3420–3427.
[15] a) J. Ehrmaier, E. J. Rabe, S. R. Pristash, K. L. Corp, C. W. Schlenker, A. L. Sobolewski, W. Domcke, *J. Phys. Chem. A* **2019**, *123*, 8099–8108; b) W. Domcke, A. L. Sobolewski, C. W. Schlenker, *J. Chem. Phys.* **2020**, *153*, 100902.
[16] M. M. Roessler, E. Salvadori, *Chem. Soc. Rev.* **2018**, *47*, 2534–2553.
[17] S. Richert, C. E. Tait, C. R. Timmel, *J. Magn. Reson.* **2017**, *280*, 103–116.
[18] Y. Wang, A. Vogel, M. Sachs, R. S. Sprick, L. Wilbraham, S. J. A. Moniz, R. Godin, M. A. Zwijnenburg, J. R. Durrant, A. I. Cooper, J. Tang, *Nat. Energy* **2019**, *4*, 746–760.
[19] G. Filippini, F. Longobardo, L. Forster, A. Criado, G. Di Carmine, L. Nasi, C. D'Agostino, M. Melchionna, P. Fornasiero, M. Prato, *Sci. Adv.* **2020**, *6*, eabc9923.
[20] F. Longobardo, G. Gentile, A. Criado, A. Actis, S. Colussi, V. Dal Santo, M. Chiesa, G. Filippini, P. Fornasiero, M. Prato, M. Melchionna, *Mater. Chem. Front.* **2021**, *5*, 7267–7275.
[21] C. Riplinger, J. P. Y. Kao, G. M. Rosen, V. Kathirvelu, G. R. Eaton, S. S. Eaton, A. Kutateladze, F. Neese, *J. Am. Chem. Soc.* **2009**, *131*, 10092–10106.
[22] C. E. Tait, P. Neuhaus, H. L. Anderson, C. R. Timmel, *J. Am. Chem. Soc.* **2015**, *137*, 6670–6679.
[23] W. Wei, T. Jacob, *Phys. Rev. B* **2013**, *87*, 085202.
[24] C. Merschjann, T. Tyborski, S. Orthmann, F. Yang, K. Schwarzburg, M. Lublow, M.-Ch. Lux-Steiner, Th. Schedel-Niedrig, *Phys. Rev. B* **2013**, *87*, 205204.
[25] A. Ugolotti, C. Di Valentin, *Appl. Surf. Sci.* **2023**, *608*, 155164.
[26] C. Franchini, M. Reticcioli, M. Setvin, U. Diebold, *Nat. Rev. Mater.* **2021**, *6*, 560–586.
[27] D. L. Meyer, F. Lombeck, S. Huettner, M. Sommer, T. Biskup, *J. Phys. Chem. Lett.* **2017**, *8*, 1677–1682.
[28] G. Ricci, E. San-Fabián, Y. Olivier, J. C. Sancho-García, *ChemPhysChem* **2021**, *22*, 553.
[29] J. Li, Z. Li, H. Gong, J. Zhang, Y. Yao, Q. Guo, *Front. Chem.* **2022**, *10*, 999856.
[30] L. Tučková, M. Straka, R. R. Valiev, D. Sundhilm, *Phys. Chem. Chem. Phys.* **2022**, *24*, 18713–18721.
[31] M. Re Fiorentin, F. Risplendi, M. Palummo, G. Cicero, *ACS Appl. Nano Mater.* **2021**, *4*, 1985–1993.
[32] R. Godin, Y. Wang, M. A. Zwijnenburg, J. Tang, J. R. Durrant, *J. Am. Chem. Soc.* **2017**, *139*, 5216–5224.
[33] S. Weber, *eMagRes* **2017**, *6*, 255–270.
[34] A. Privitera, E. Macaluso, A. Chiesa, A. Gabbani, D. Faccio, D. Giuri, M. Briganti, N. Giaconi, F. Santanni, N. Jarmouni, L. Poggini, M. Mannini, M. Chiesa, C. Tomasini, F. Pineider, E. Salvadori, S. Carretta, R. Sessoli, *Chem. Sci.* **2022**, *13*, 12208–12218.
[35] S. Stoll, A. Schweiger, *J. Magn. Reson.* **2006**, *178*, 42–5.
[36] C. E. Tait, M. D. Krzyaniak, S. Stoll, *J. Magn. Reson.* **2023**, *349*, 107410.
[37] S. V. Nurhayati, A. Alni, A. A. Nugroho, Y. Majima, S. Lee, Y. P. Nugraha, H. Uekusa, *J. Phys. Chem. A* **2020**, *124*, 2672–2682.
[38] Y. Kang, Y. Yang, L. Yin, X. Kang, G. Liu, H.-M. Cheng, *Adv. Mater.* **2015**, *27*, 4572–4577.
[39] J. Telser, *eMagRes* **2017**, *6*, 207–234.
[40] F. Metz, S. Friedrich, G. Hohlneicher, *Chem. Phys. Lett.* **1972**, *16*, 353–358.
[41] D. A. Antheunis, J. Schmidt, J. H. van der Waals, *Mol. Phys.* **1974**, *27*, 1521–1541.
[42] R. H. Clarke, R. E. Connors, T. J. Schaafsma, J. F. Kleibeuker, R. J. Platenkamp, *J. Am. Chem. Soc.* **1976**, *98*, 3674–3677.
[43] Y. Xu, S.-P. Gao, *Int. J. Hydrogen Energy* **2012**, *37*, 11072.
[44] P. Liu, P. Longo, A. Zaslavsky, D. Pacifici, *J. Appl. Phys.* **2016**, *119*, 014304.
[45] P. Makuła, M. Pacia, W. Macyk, *J. Phys. Chem. Lett.* **2018**, *9*, 6814–6817.

Manuscript received: September 12, 2023
Accepted manuscript online: October 6, 2023
Version of record online: October 23, 2023